The observation of nonlinear ion cyclotron wave excitation during high-harmonic fast wave heating in the large helical device[a)]

H. Kasahara,[1,b)] T. Seki,[1] R. Kumazawa,[1] K. Saito,[1] T. Mutoh,[1] S. Kubo,[1] T. Shimozuma,[1] H. Igami,[1] Y. Yoshimura,[1] H. Takahashi,[1] I. Yamada,[1] T. Tokuzawa,[1] S. Ohdachi,[1] S. Morita,[1] G. Nomura,[1] F. Shimpo,[1] A. Komori,[1] O. Motojima,[1] T. Oosako,[2] Y. Takase,[2] Y. Zhao,[3] and J. Kwak[4]
[1]*National Institute for Fusion Science, Toki 509-5292, Japan*
[2]*Graduate School of Frontier Sciences, University of Tokyo, Kashiwa 277-8561, Japan*
[3]*Institute of Plasma Physics, Academia Sinica, Hefei 230031, People's Republic of China*
[4]*Korea Atomic Energy Research Institute, Dajeon 305-600, Republic of Korea*

(Presented 13 May 2008; received 11 May 2008; accepted 25 July 2008; published online 31 October 2008)

A wave detector, a newly designed magnetic probe, is installed in the large helical device (LHD). This wave detector is a 100-turn loop coil with electrostatic shield. Comparing a one-loop coil to this detector, this detector has roughly constant power coupling in the lower frequency range of 40 MHz, and it can easily detect magnetic wave in the frequency of a few megahertz. During high-harmonic fast wave heating, lower frequency waves (<10 MHz) were observed in the LHD for the first time, and for the power density threshold of lower frequency wave excitation (7.5 MHz) the power density of excited pumped wave (38.47 MHz) was approximately −46 dBm/Hz. These lower frequencies are kept constant for electron density and high energy particle distribution, and these lower frequency waves seem to be ion cyclotron waves caused by nonlinear wave-particle interaction, for example, parametric decay instability. © *2008 American Institute of Physics.*
[DOI: 10.1063/1.2973325]

I. INTRODUCTION

High-harmonic fast wave (HHFW) heating has been investigated in high beta regime, and the accessibility and electron absorption have been inspected in torus plasmas such as spherical tokamak.[1,2] In electron heating experiments using HHFW in NSTX (injected HHFW power is less than 4.3 MW, and the excited frequency is 30 MHz), the temperature of the hot ion component is observed using charge exchange and recombination spectroscopy.[3] The excited wave frequency is typically ten times larger than the ion cyclotron range of frequencies (ICRF), and ion cyclotron damping is negligible in the experimental region. When the ion temperature at the plasma edge is directly increased, an ion Bernstein wave (IBW) is detected by Langmuir probe measurements. Due to a nonlinear wave coupling process in parametric decay instability (PDI), three-wave coupling, the launched HHFW is transformed into an ion cyclotron quasimode (ICQM) of slow wave and an IBW of electrostatic wave.

The large helical device (LHD) is a superconducting magnetic confinement device with heliotron configuration, the world's largest helical device, and high electron beta is capable of achieving normalized beta of 5%. Three pairs of ICRF heating antennas are installed at three toroidal sections in the LHD (3.5 U & L, 4.5 U & L, and 7.5 U & L), and two pairs of them (3.5 U & L and 7.5 U & L) are used for ICRF steady state operation and minority ICRF heating experiments.[4,5] A HHFW electron heating experiment was attempted in the LHD with normalized beta of 1% (magnetic field B of 1.5 T at major radius R of 3.6 m), and central electron heating was clearly achieved when additional electron cyclotron heating was injected at the core region of plasma.[6] In some parts of the experiment an extended ion tail was observed, and ion heating was carried out in HHFW electron heating experiments. Second ion cyclotron resonances of hydrogen exists at near $r/a \sim 0.6$, and second hydrogen cyclotron damping is a strong candidate to be the ion heating mechanism, rather than nonlinear wave-particle interaction like PDI.[7] It is important to clarify the parasitic ion heating mechanism in HHFW electron heating experiments, and a high-sensitivity wave measurement system using a newly designed wave detector to measure these waves was installed in the LHD.

II. EXPERIMENTAL SETUP OF WAVE DETECTION

This detector, which consists of 100-turn loop coil (see Fig. 1), 4 layers by 25 lines, is installed between the chamber wall and wall armer plates in the vacuum vessel of the LHD, and it can detect excited electromagnetic wave which propagates across plasma in front of the HHFW heating antenna at the 3.5 port (see Fig. 2). The diameter of the loop coil line is less than 0.5 mm, and the cross section of this loop coil is approximately 88 mm^2, 22×4 mm^2. The total length of the loop line at the detector is approximately 5.2 m, and this length is significant because it is longer than the wavelength

[a)]Contributed paper, published as part of the Proceedings of the 17th Topical Conference on High-Temperature Plasma Diagnostics, Albuquerque, New Mexico, May 2008.
[b)]Electronic mail: kasahara.hiroshi@lhd.nifs.ac.jp.

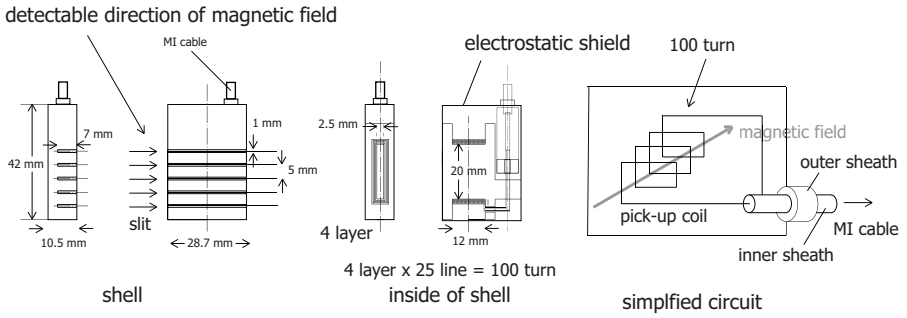

FIG. 1. The wave detector consists of a 100-turn loop coil, 4 layers by 25 lines, and a metal shell for an electrostatic shield, with five slits for electromagnetic coupling. The width of these slits is narrow (~1 mm), and the directionality to these slits for electromagnetic coupling is stronger than that of the perpendicular direction. In the lower frequency region (<40 MHz), the detectable power coupling of this detector is more constant than the detected power coupling of a one-turn loop coil except at the self-resonant frequency of the coil.

in the frequency of 50 MHz. According to a mock-up test of the detector, total resistance is approximately 2 Ω, and inductance is roughly 100 μH under 10 MHz. The inductance of this detector is not changed in the range of frequency (<40 MHz), and the power coupling in the range of frequency (<100 MHz) is more constant than that of the one-turn loop coil. This detector has a narrow self-resonant frequency of 20 MHz due to the large inductance value of a 100-loop coil, and the power coupling efficiency at 20 MHz is stronger than the efficiency around the self-resonant frequency (Fig. 3). Although there is self-resonant frequency in the measured frequency range (0–40 MHz), this resonant frequency is not near experimental observed frequency peaks.

The detector is covered with an all-metal shield having slits for electromagnetic coupling, and electrostatic wave is strongly reduced. Because the slit width is narrow (~1 mm), the directionality of electromagnetic coupling to the slit is good and the coupling effect to vertical direction of slit is negligible. The slit direction is not the same aligned with direction to poloidal magnetic field, but is the same aligned with direction to the direction of the gag between the wall armor plates. The difference between the poloidal magnetic field and the slit is 13°, and the wave coupling coefficient to poloidal magnetic filed direction is approximately 0.97. The wave coupling coefficient in the toroidal magnetic field direction is approximately 0.22, and it must be significant in the case of strong wave excitation in the direction of the toroidal magnetic field. Absolute power and phase calibration of this detector have not been finished, and for the accurate quantitative estimation of detected wave power of various frequencies these calibration are needed.

The cable length between the wave detector and measurement system is roughly 300 m, and the loss of a coaxial line must be significant in the frequency region. Furthermore, if the pumped wave power is much stronger than the excited lower frequency power, lower frequency wave detection is difficult because a high-gain and high-resolution power measurement system is needed. A real-time spectrum analyzer (Tektronix RSA3408A) is a useful system for measuring these lower waves and the pumped waves at the same time. The measurable frequency of RSA3408A is from dc to 8 GHz, and detectable power range is from −150 to +10 dBm. The acquisition time length is a maximum 1.26 s

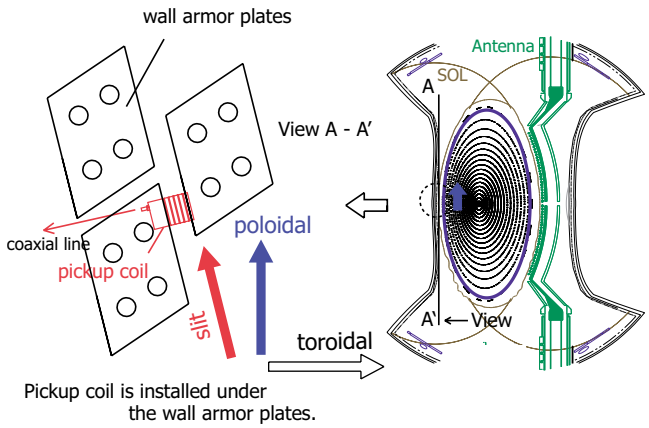

FIG. 2. (Color online) The wave detector is installed at the same toroidal section as the HHFW heating antenna at the 3.5 port in the LHD, and the detector is between chamber wall and wall armor plate at the opposite side wall of HHFW excitation antenna. The direction of detector slits is roughly the same direction as the poloidal direction; the difference between poloidal direction and slit direction is 13°.

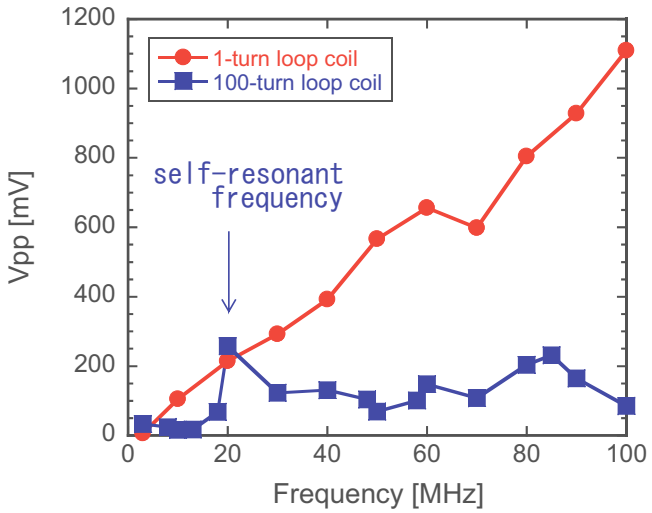

FIG. 3. (Color online) Differences in wave power coupling characteristic between 1-turn loop coil and 100-turn loop coil. The vertical axis is the detected voltage which is measured by 1-turn loop coil and 100-turn loop coil, and the horizontal axis is the source wave frequency. The coupling efficiency of the 1-turn loop coil increases as frequency is increased. In the 100-turn loop coil, the power coupling efficiency in a wide range of frequency (0–100 MHz) is more constant than that of the 1-turn loop coil.

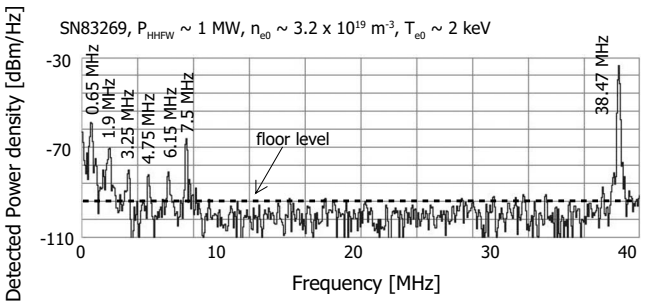

FIG. 4. Lower frequency waves (<10 MHz) are observed during HHFW heating, and the pumped wave frequency is 38.47 MHz. The difference of the observed power density level between the pumped wave and the detected lower frequency wave (frequency of 7.5 MHz) is approximately −40 dB/Hz, and the noise power level is approximately −95 dBm/Hz.

(256 MB), when the measurable frequency is selected between dc and 40 MHz on real-time spectrum analyzing mode.

III. THE CHARACTERISTIC OF OBSERVED LOWER FREQUENCY WAVES

Figure 4 shows electromagnetic waves using the real-time spectrum analyzer measurement during HHFW heating, and the frequency of 38.47 MHz is the pumped wave frequency using HHFW heating antenna excitation with the injected power of $P_{\mathrm{HHFW}} \sim 1$ MW. In this discharge (SN83269), the plasma parameters are as follows: Line averaged electron density n_{e0} of 3.2×10^{19} m^{-3} at $R=3.67$ m, electron temperature of $T_{e0}=2$ keV at $R=3.6$ m, and the minority ratio of hydrogen is approximately 20% using spectroscopy measurement in helium discharge. In the lower frequency range from dc to 10 MHz, clear frequency peaks are observed, and the frequency peak at 7.5 MHz is an ordinary strong peak. These lower frequency peaks do not change for electron densities from 1.7×10^{19} to 1.1×10^{19} m^{-3}, and the appearance of these lower frequency waves is not related to high energy particle distribution because there is little difference between lower frequency discharges and only pumped wave discharges in the high energy particle distribution measured by SiFNA. In the power modulation experiments, these lower frequency waves vanish at the same time after HHFW injection is stopped. This shows that these lower frequency waves are not some kind of high energy particle driven Alfvén wave or ion cyclotron emission.[8] To explain this lower frequency excitation, some nonlinear wave-particle interaction such as PDI is required. Assuming that the daughter waves of these lower frequency waves are IBW, the daughter wave caused by PDI cannot be detected by this detector because IBW is an electrostatic wave. Even if ICQM as lower-sideband daughter wave is excited around a frequency of 30 MHz, it is difficult for it to propagate to this detector because there are cyclotron resonance and an L cutoff layer around the detector with high magnetic field. Solving the ion cyclotron wave (ICW) dispersion relation in experimental parameters, lower frequency waves (<10 MHz) are excited around magnetic field B of 1 T at plasma edge, which is consistent with the observed lower frequencies.

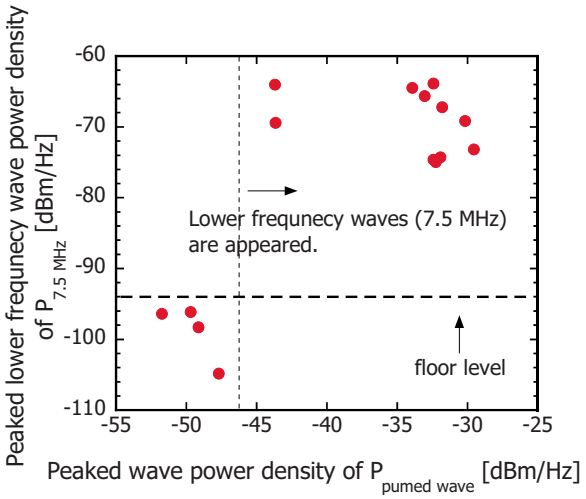

FIG. 5. (Color online) A clear power density threshold of the lower frequency wave (7.5 MHz) appearance is observed for the case of the pumped wave (38.47 MHz), and the threshold power density level is approximately −46 dBm/Hz.

Although these lower frequency waves are not always observed during HHFW heating, they are detected at an injected power of ~1 MW. In these observed discharges, plasma parameters have a variety of injected HHFW power, injected neutral beam power, electron density, and a minority ratio of hydrogen to helium. The observed pumped wave power density level plays a key role in exciting these lower frequency waves. Figure 5 shows the appearance of lower frequency waves for observed pumped wave power density level. The horizontal axis is the peaked power density level of the pumped wave (38.47 MHz), and the vertical axis is that of the lower frequency wave (7.5 MHz). The floor power density level is approximately −94 dBm/Hz, and the difference of power density level at which lower frequency waves appear is roughly 20 dB. When the power density level of the pumped wave is decreased to −46 dBm/Hz, these lower frequency waves vanish. There is a clear power density threshold of the appearance of this lower frequency wave excitation for the power density of the pumped wave.

IV. SUMMARY

A newly designed magnetic coil (100-turn loop coil) having a good directionality to electromagnetic wave coupling and including an electrostatic shield is installed in the LHD, and lower frequency waves are observed during a HHFW heating experiment. Considering these lower frequency waves are not related to electron density and high energy particle distribution, they seem to be an ICQM caused by PDI process. Moreover there is a clear power density threshold of the appearance of these lower frequency waves for the pumped wave power density, and these lower frequencies are consistent with the ICW frequency which is excited around magnetic field of 1 T at the plasma edge.

ACKNOWLEDGMENTS

This work has been partly supported by a Grant-in-Aid for Scientific Research from MEXT, and all work is sup-

ported by NIFS through the following budget codes: NIFS07ULRR06, NIFS07ULRR07, and NIFS07ULRR08.

[1] B. P. LeBlanc, R. E. Bell, S. M. Kaya, D. Stutman, M. G. Bell, M. L. Bitter, C. Bourdelle, D. A. Gates, R. Maingi, S. S. Medley *et al.*, Nucl. Fusion **44**, 513 (2004).
[2] T. Yamada, A. Ejiri, Y. Shimada, T. Oosako, J. Tsujimura, Y. Takase, and H. Kasahara, Rev. Sci. Instrum. **78**, 083502 (2007).
[3] T. M. Biewer, R. E. Bell, S. J. Diem, C. K. Phillips, J. R. Wilson, and P. M. Ryan, Phys. Plasmas **12**, 056108 (2005).
[4] T. Mutoh, R. Kumazawa, T. Seki, K. Saito, F. Shimpo, G. Nomura, T. Watari, X. Jikang, G. Cattanei, H. Okada *et al.* Plasma Phys. Controlled Fusion **42**, 265 (2000).
[5] R. Kumazawa, T. Mutoh, T. Seki, K. Saito, T. Watari, Y. Nakamura, M. Sakamoto, T. Watanabe, S. Kubo, T. Shimozuma *et al.*, Plasma Phys. Controlled Fusion **8**, 28 (2006).
[6] H. Kasahara, T. Oosako, Y. Takase, N. Takeuchi, K. Saito, T. Seki, T. Mutoh, R. Kumazawa, and LHD Experimental Group, J. Korean Phys. Soc. **49**, S192 (2006).
[7] M. Porkolab, Phys. Fluids **20**, 2058 (1977).
[8] K. G. McClements, C. Hunt, R. O. Dendy, and G. A. Cottrell, Phys. Rev. Lett. **82**, 2099 (1999).